# ON THE SPECTRAL RESOLUTION REQUIREMENTS FOR THE DERIVATION OF LEAF AREA INDEX FROM HYPERSPECTRAL REMOTE SENSING DATA

T. Peisker [a], D. Spengler [a], K. Segl [a], L. Guanter [a], H. Kaufmann [a]

[a]GFZ, Helmholtz Centre Potsdam - German Research Centre for Geosciences, Telegrafenberg, 14473 Potsdam, Germany (tpeisker,daniel,segl,luisguan,charly)@gfz-potsdam.de

**KEY WORDS:** reflectance simulation, spectral band, leaf area index, sensor simulation, EnMAP

**ABSTRACT:**

This paper presents a sensitivity analysis to find the optimal spectral band configuration for the derivation of leaf area index (LAI) from hyperspectral remote sensing data. The analysis is carried out on a data base of canopy reflectance spectra with a very high spectral sampling rate accompanied with their true LAI. The reflectance spectra are simulated by a ray tracing software from three dimensional (3D) crop canopy models containing field measured spectra of plant parts. Empirical models are used to derive relationship between LAI and selected widely used vegetation indices. Best correlation results have been obtained with indices based on a 2-band-model (red, near infrared (NIR)), whereas the position of the NIR band should be located between the red edge inflection point and the lower red shoulder. Binning bands to broad bands improves the correlations due to reduced noise.

## 1. INTRODUCTION

The derivation of biophysical variables from multispectral optical Earth Observation (EO) data is a proven way to obtain information about the observed surface in a fast manner and on a large scale. In the near future hyperspectral instruments like the upcoming Environmental Mapping & Analysis Program (EnMAP) (launch scheduled for 2013) will provide a new quality of space-borne optical EO data which signifies highly spectral sampled data on a large scale. These data are expected to further increase the accuracy of the retrieval result. Hence, it is useful to know the spectral configuration requirements for a given application, such as band selection, spectral binning, and sensor optimisation.

As a first example, this study was undertaken to investigate the optimal spectral bands and methods for the derivation of Leaf Area Index (LAI) from hyperspectral remote sensing data.

The LAI is an important biophysical variable to asses the state and vitality of vegetation as it is directly related to photosynthesis, transpiration, evapotranspiration, and net primary production. Furthermore, it is used as a key parameter for regional and global ecosystem models (Scurlock et al., 2001).

## 2. DATA SIMULATION

The data for the analysis were modelled from virtual canopies. Simulating artificial spectra enables to include numerous variations that can not be obtained from measurements in the field.

The canopy spectra was simulated by utilizing ray tracing software (Lewis, 1999) from 3D canopy models superposed with in situ spectra, i.e. plant parts and soil samples (Peisker et. al., 2008).

### 2.1 3D canopy model

A virtual 3D canopy model is generated by using 3D plant models, soil background information including a soil digital elevation model (DEM) and the distribution of the plants within the canopy. Furthermore, a spectral library containing spectral information of the plant organs and the soil is essential.

**2.1.1 3D plant model:** The Software AMAPsim (Barczi et al., 2007) was used for plant simulation providing a tool to reconstruct plants virtually based on real measurements. The software contains a structural growth model based on botanical theory to simulate plant morphogenesis producing accurate, complex and detailed plant architectures. Shape parameters of the plant organs leaves, stems and ears were acquired at different growth stages to define the organ sizes and their growth dynamics (Barczi et al., 2007).

**2.1.2 3D soil model and canopy geometry:** A data base of field-measured height profiles was used to generate a soil DEM with the typical geometry and distance of furrows within rye fields due to mechanical drilling of seed. The plant models were distributed within the soil model by cloning and randomly rotating the 'master plant' around its vertical axis (Lewis, 1999). The distance between the furrows and the number of plants placed within a defined section of a furrow defines the plant density of the canopy.

### 2.2 Canopy reflectance simulation

Canopy reflectance data is determined by the acquisition and illumination geometry as well as the geometry and spectral information of the objects on the surface. To obtain these mixed spectra the artificial 3D crop field is measured virtually by ray tracing. Ray tracing is a method to generate two dimensional (2D) image data by tracing the path of light through a 3D scene onto an image plane (Glassner, 1989).

The canopy reflectance of the virtual 3D rye canopy is modelled by the Advanced RAdiometric RAy Tracer (ARARAT) developed by Philip Lewis (Lewis, 1999; Lewis & Muller, 1992). The ray tracer calculates the canopy reflectance based on 3D canopy descriptions with associated spectral information, camera imaging properties and illumination conditions by using reverse ray tracing (Lewis, 1999).

## 3. DATA BASE

A spectral library with about 250 different spectra of winter rye was built up. The spectra were sampled from canopies within one growth stage with slightly less or more developed plants but varying in their geometry (distance between drilling rows, orientation of drilling rows), plant appearance (number of tillers at all, number of fully developed tillers) and soil properties (soil moisture) to adapt the possible conditions within several fields. Figure 1 illustrates the variations within the data base of simulated reflectance spectra of winter rye canopies.

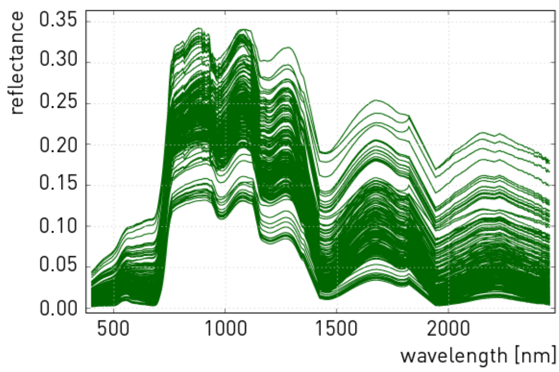


Figure 1. Canopy variations: All simulated reflectance spectra of different winter rye canopies.

Besides the spectral library of the canopy spectra, the true LAI of the canopies was calculated as part of the data base. The LAI is the functional one-sided (green) leaf area (s) per unit ground area (G) (Monteith, 1973).

$$LAI = \frac{s}{G} \left[ \frac{m^2}{m^2} \right] \quad (1)$$

The LAI was calculated by summing the facets' area of the leaves of the 3D canopy normalised by the horizontal area of the 3D soil surface which ensures real measured LAI for each canopy spectrum. The LAI for the spectra of the data base are between 0.9 and 3.5.

## 4. ANALYSIS METHODS

To find the optimal spectral bands for LAI retrieval, numerous reflectance spectra were calculated from each spectrum of the data base applying spectral response functions with varying widths and positions as well as noise within an end-to-end sensor simulation (section 4.1). Finally, empirical models are used to derive the relation between the LAI and selected widely used vegetation indices (section 4.2).

### 4.1 End-to-end sensor simulation

Each reflectance spectrum of the data base was transformed to digital numbers (DN) following a forward simulation approach. It consisted in three steps:

- Conversion of reflectance data to top-of-atmosphere-radiance (TOA-radiance) data with tabled data calculated from MODTRAN4,
- Spectral resampling using defined spectral band setting given by a set of spectral response function spectral sampling interval and band width,
- Radiometric simulation including noise (Gaussian-distributed) and quantisation to $2^{12}$ bits.

TOA-radiance conversion was carried out using MODTRAN4 which required location specific input parameters, i.e. illumination and observation angles, columnar water vapour (CWV), aerosol optical thickness (AOT), and surface elevation (Guanter et al. 2007). The illumination was chosen to adapt the conditions of a summer day during noon in the region of Brandenburg (latitude = 52.5°, longitude = 13°, sun zenith angle = 35°, sun azimuth angle = 170°). The viewing was defined to be nadir with a height of 700 kilometres. For the AOT and the CWV mean values of a representative summer day (AOT = 0.2 at 550 nm, CWV = 2.0 g/cm$^2$) were chosen.

Spectral resampling was carried out for each spectrum of the data base while various spectral response functions were applied. Full width of half maximum (FWHM) was applied to a sequence between 5 nm and 130 nm using 5 nm increments with an additional lowest band width of 2nm (2, 5, 10 ... 130 nm). The band's centre position was stepwise altered between meaningful limits for each band (e.g. red band: 600 - 740 nm in 5 nm steps). Hence, more than 750 different spectral band configurations for each band have been tested.

The radiometric simulation was performed with two different noise levels (well and bad) to get an impression of noise effects. Therefore, noise equivalent radiance (NER) was calculated twice, resolving reflectance data to 0.35 % of the signal (well) and to 2.5 % of the signal (bad) at bands with a FWHM of 5 nm (Schläpfer & Schaepman, 2002). Bands with a FWHM larger than 5 nm had to adapt leading to improved signal-to-noise ratios (SNR) due to recording of higher amounts of photons (table 1).

| FWHM | SNR well | SNR bad |
|---|---|---|
| 5 nm | ~ 350 | ~ 85 |
| 10 nm | ~ 500 | ~ 125 |
| 20 nm | ~ 700 | ~ 170 |
| 50 nm | ~ 1100 | ~ 275 |

Table 1. SNR values for selected FWHMs for well and bad noise configurations at 800 nm and 0.3 reflectance level.

To accomplish the end-to-end sensor simulation an atmospheric correction was performed to retrieve reflectance data from DN data.

### 4.2 Leaf area index retrieval

The retrieval of the LAI is done conventionally using empirical relationship between LAI and vegetation indices (Baret & Guyot, 1991; Haboudane et al., 2004). Therefore, 31 widely used vegetation indices were applied to both broad-band (i.e. NDVI, SR, RDVI, greenNDVI, etc.) and narrow-band indices (i.e. REIP, DVI, GI, etc.). Each index is correlated with the true LAI using second order polynomial, exponential, logarithmic and power regression models. For each band configuration a single model was developed. Table 2 shows all vegetation indices with a strong relationship to LAI in this study for a selected band configuration.

| VI | Reference | $R^2$ | Bands |
|---|---|---|---|
| WDRVI | Gitelson, 2004 | 0.937 | B2, B4 |
| GreenNDVI | Bushman & Nagel, 1993; Gitelson & Merzylak, 1994 | 0.937 | B1, B4 |
| MSR | Chen, 1996 | 0.937 | B2, B4 |
| SR | Birth & McVey, 1968; Jordan, 1969 | 0.935 | B2, B4 |
| NDVI | Rouse et al., 1973 | 0.930 | B2, B4 |
| PSNDa | Blackburn, 1998 | 0.930 | B2, B4 |
| GI | Smith et al., 1995 | 0.928 | B1, B2 |
| TVI | Deering et al., 1975 | 0.927 | B2, B4 |
| CTVI | Perry & Lauten-schlager, 1984 | 0.925 | B2, B4 |
| ChlNDI | Gitelson & Merzylak, 1994 | 0.903 | B3, B5 |
| ZTM | Zarco-Tejada et al., 2001 | 0.902 | B3, B5 |
| mNDVI | Jürgens, 1997 | 0.899 | B4, B6 |
| MSI | Rock et al., 1986 | 0.898 | B4, B6 |
| CIgreen | Gitelson et al., 2003 | 0.894 | B1, B4 |

Table 2. Vegetation indices with a strong relationship ($R^2$ over 0.85) with LAI for a selected spectral band configuration with well noise configuration: FWHM = 20 nm for all bands, B1 centre = 550 nm, B2 centre = 670 nm, B3 centre = 705 nm, B4 centre = 800 nm, B5 centre = 750 nm, B6 centre = 1670 nm.

The best fitting model, describing the relationship between WDRVI and LAI, determined by the coefficient of determination $R^2$ (3-73 from Wälder, 2008) using cross validation was chosen for the subsequence analysis.

## 5. RESULTS

### 5.1 Optimal spectral band settings

Polynomial models which were found to provide the best description of the relationship between WDRVI and LAI were calculated for each spectral band configuration in the red and NIR range. The results are presented in figure 2.

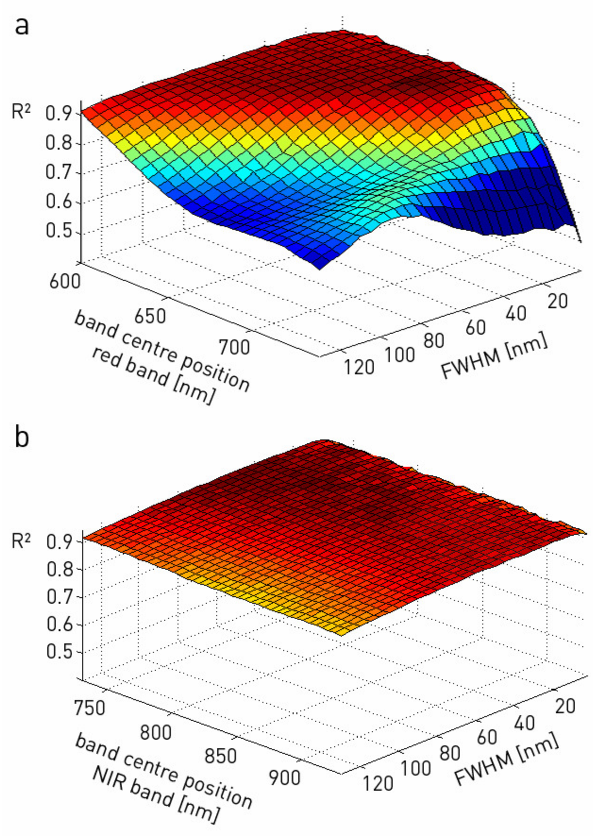


Figure 2. $R^2$ of best regression model between WDRVI and LAI for all calculated spectral band configurations of red band (a) and NIR band (b) with well noise configuration.

The best band setting for the red band is a FWHM of about 10 - 30 nm and the centre position at 670 - 680 nm which is the position of the chlorophyll absorption band. Remarkable is the best location of the NIR band centre between 740 and 800 nm which is the range between the red edge inflection point and the lower red shoulder. However, one would suspect the top of the red shoulder as best. The FWHM is varying between 20 and 70 nm depending on the location.

All presented results were achieved for well noise configuration. With the spectra with bad SNRs no good fitting of the regression models could be achieved ($R^2$ less than 0.85).

### 5.2 Binning

As shown in the previous section, noise is a strong limiting factor. Narrow bands are noisier than broad bands (table 1). Hence, binning narrow bands to broad bands reduces noise and increases the SNR.

As an example, 4 nm sampled spectra with different noise configuration were compared. For the best bands the regression model fits with 93.1 % ($R^2$ = 0.931) for well and 82.2 % for bad noise configurations. The binning was calculated by averaging the sum of the band values. Figure 3 shows the binning results where the best combination of binned bands resulted with a fitting of 93.1 %.

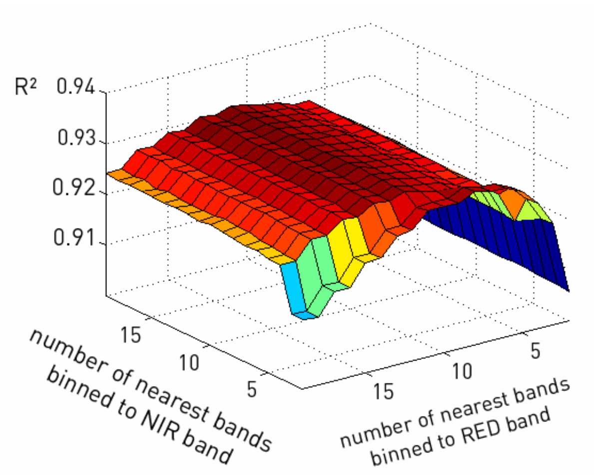


Figure 3. $R^2$ of best regression model between WDRVI and LAI for binned bands of 4 nm sampled spectra with bad noise configuration. Centre for red band = 680 nm, centre for NIR band = 780 nm.

Binning spectra with high SNR values also improves the prediction of LAI. EnMAP spectra, for example, predict with a $R^2$ = 0.93 (red band: centre ≅ 672 nm, FWHM ≅ 6.5 nm; NIR band: centre ≅ 786 nm, FWHM ≅ 7.5 nm). Binning the bands weighted yields with a $R^2$ of 0.936.

## 6. CONCLUSION

This study was conducted to investigate the optimal spectral bands for the retrieval of LAI. The WDRVI model was found to be the best to predict LAI. The optimal bands are a red band with FWHM of about 10 - 30 nm located between 670 and 680 nm, and a NIR band with a FWHM of about 20 - 70 nm depending on the location between 740 and 800 nm. Predicting LAI from hyperspectral data yields equal results as with optimal broad bands. However, the possibility of binning bands enables the adaption of the best band setting leading to improved retrieval results over optimal broad bands.

## ACKNOWLEDGEMENTS

This work is part of the EnMAP project funded by the German Federal Ministry for Education and Research (BMBF) / Federal Ministry of Economics and Technology (BMWi). We thank the AGRAR GbR Wittbrietzen and the Faculty of Agriculture and Horticulture of the Humboldt-University Berlin enabling the data collection. Furthermore we thank Jean-Francois Barczi supporting us with the generation of the 3D plant models and Philip Lewis for providing the ARARAT software and additional help.

## REFERENCES


Barczi, J.-F.; Rey, H.; Caraglio, Y; De Refeye, P.; Barthélémy, D.; Xue Dong, Q. & Fourcaus, T., 2007. AmapSim: A structural whole-plant simulator based on botanical knowledge and designed to host external functional models. *Annals of Botany*, pp. 1-14.

Baret, F. & Guyot, G., 1991. Potential and Limits of Vegetation Indices for LAI and APAR Assessment. *Remote Sensing of Environment*, 35, pp. 161-173.

Gitelson, A.A., 2004. Wide dynamic range vegetation index for remote quantification of biophysical characteristics of vegetation. *Journal of Plant Physiology,* 161, pp. 165-173.

Glassner, A.S., 1989. *An Introduction to Ray tracing.* Academic Press Ltd., London.

Guanter, L.; Richter, R. & Kaufmann, H., 2007. On the application of the MODTRAN4 atmospheric radiative transfer code to optical remote sensing. *International Journal of Remote Sensing,* in press.

Haboudane, D.; Miller, J.R.; Pattey, E.; Zarco-Tejada, P.J. & Strachan, I.B., 2004. Hyperspectral vegetation indices and novel algorithms for predicting green LAI of crop canopies: Modeling and validation in the context of precision agriculture. *Remote Sensing of Environment*, 90, pp. 337-352.

Kaufmann, H.; Segl, K.; Guanter, L.; Hofer, S.; Foerster, K.-P.; Stuffler, T.; Mueller, A.; Richter, R.; Bach, H.; Hostert, P. & Chlebek, C., 2008. Environmental Mapping and Analysis Programm (EnMAP) – Recent Advances and Status. *Proc IGARSS 2008, IEEE International*, Boston.

Lewis, P., 1999. The Botanical Plant Modelling System. *Agronomie: Agriculture and Environment*, 19, pp.185-210.

Lewis, P. & Muller, J.-P., 1992. The Advanced Radiometric Ray Tracer: ARARAT for Plant Canopy Reflectance Simulation. *Proc ISPRS '92*, Washington D.C.

Monteith, J.L., 1973. *Principles of Environmental Physics.* Edward Arnold, London.

Peisker, T.; Spengler, D.; Segl, K.; Itzerott, S. & Kaufmann, H., 2008. Simulation of hyperspectral reflectance data using artificial 3D crop fields. In: Ehlers, M.; Behnke, K.; Gerstengarbe, F.-W.; Hillen, F.; Koppers, L.; Stroink, L.; Wächter, J. (Eds.) *Digital Earth Summit on Geoinformatics 2008: Tools for Global Change Research*, pp. 39-44.

Rouse, J.W.; Haas, R.H.; Schell, J.A. & Deering, D.W., 1973. Monitoring vegetation systems in the Great Plains with ERTS, Proceedings of the *Third Earth Resources Technology Satellite-1 Symposium,* NASA, Greenbelt, MD, pp. 301-317.

Schläpfer, D. & Schaepman, M., 2002. Modeling The Noise Equivalent Radiance Requirements of Imaging Spectrometers Based On Scientific Applications. *Applied Optics*, 41, pp. 5691-5701.

Scurlock, J. M. O.; Asner, G. P. & Gower, S. T., 2001. Worldwide Historical Estimates of Leaf Area Index, 1932-2000. ORNL Memorandum ORNL/TM-2001/268, Oak Ridge National Laboratory, Oak Ridge, Tennesse, USA.

Wälder, O., 2008. *Mathematical methods for engineers and geoscientists.* Springer-Verlag, Berlin Heidelberg, pp. 85.